

University of Dundee

## Controlled metallization of ion-exchanged glasses by thermal poling

Reduto, Igor; Babich, Ekaterina ; Zolotovskaya, Svetlana A.; Abdolvand, Amin; Lipovskii, Andrey; Zhurikhina, Valentina

*Published in:*  
Journal of Physics: Condensed Matter

*DOI:*  
[10.1088/1361-648X/ac276c](https://doi.org/10.1088/1361-648X/ac276c)

*Publication date:*  
2021

*Licence:*  
CC BY

*Document Version*  
Peer reviewed version

[Link to publication in Discovery Research Portal](#)

### *Citation for published version (APA):*

Reduto, I., Babich, E., Zolotovskaya, S. A., Abdolvand, A., Lipovskii, A., & Zhurikhina, V. (2021). Controlled metallization of ion-exchanged glasses by thermal poling. *Journal of Physics: Condensed Matter*, 33(50), [505001]. <https://doi.org/10.1088/1361-648X/ac276c>

### **General rights**

Copyright and moral rights for the publications made accessible in Discovery Research Portal are retained by the authors and/or other copyright owners and it is a condition of accessing publications that users recognise and abide by the legal requirements associated with these rights.

- Users may download and print one copy of any publication from Discovery Research Portal for the purpose of private study or research.
- You may not further distribute the material or use it for any profit-making activity or commercial gain.
- You may freely distribute the URL identifying the publication in the public portal.

### **Take down policy**

If you believe that this document breaches copyright please contact us providing details, and we will remove access to the work immediately and investigate your claim.

ACCEPTED MANUSCRIPT • OPEN ACCESS

## Controlled metallization of ion-exchanged glasses by thermal poling

To cite this article before publication: Igor Reduto *et al* 2021 *J. Phys.: Condens. Matter* in press <https://doi.org/10.1088/1361-648X/ac276c>

### Manuscript version: Accepted Manuscript

Accepted Manuscript is “the version of the article accepted for publication including all changes made as a result of the peer review process, and which may also include the addition to the article by IOP Publishing of a header, an article ID, a cover sheet and/or an ‘Accepted Manuscript’ watermark, but excluding any other editing, typesetting or other changes made by IOP Publishing and/or its licensors”

This Accepted Manuscript is © 2021 The Author(s). Published by IOP Publishing Ltd..

As the Version of Record of this article is going to be / has been published on a gold open access basis under a CC BY 3.0 licence, this Accepted Manuscript is available for reuse under a CC BY 3.0 licence immediately.

Everyone is permitted to use all or part of the original content in this article, provided that they adhere to all the terms of the licence <https://creativecommons.org/licenses/by/3.0>

Although reasonable endeavours have been taken to obtain all necessary permissions from third parties to include their copyrighted content within this article, their full citation and copyright line may not be present in this Accepted Manuscript version. Before using any content from this article, please refer to the Version of Record on IOPscience once published for full citation and copyright details, as permissions may be required. All third party content is fully copyright protected and is not published on a gold open access basis under a CC BY licence, unless that is specifically stated in the figure caption in the Version of Record.

View the [article online](#) for updates and enhancements.

## Controlled Metallization of Ion-Exchanged Glasses by Thermal Poling

Igor Reduto<sup>1,\*</sup>, Ekaterina Babich<sup>2</sup>, Svetlana Zolotovskaya<sup>3</sup>, Amin Abdolvand<sup>3</sup>, Andrey Lipovskii<sup>2</sup>, Valentina Zhurikhina<sup>2</sup>

<sup>1</sup> Institute of Photonics, Department of Physics and Mathematics, University of Eastern Finland, Joensuu 80101, Finland

<sup>2</sup> Laboratory of Multifunctional Glassy Materials, Peter the Great St. Petersburg Polytechnic University, St. Petersburg 195251, Russia

<sup>3</sup> Materials Science and Engineering Research Cluster, School of Science and Engineering, University of Dundee, Dundee DD1 4HN, UK

\*Corresponding author: Dr. Igor Reduto, igor.reduto@uef.fi, +358-504396278, Yliopistokatu 2, FI-80100 Joensuu, Finland

Dr. Ekaterina Babich, Russia, 195251, St.Petersburg, Polytechnicheskaya, 29, babich.katherina@gmail.com

Dr. Svetlana Zolotovskaya, UK, Dundee DD1 4HN, s.a.zolotovskaya@dundee.ac.uk

Dr. Prof. Amin Abdolvand, UK, Dundee DD1 4HN, A.Abdolvand@dundee.ac.uk

Dr. Prof. Andrey Lipovskii, Russia, 195251, St.Petersburg, Polytechnicheskaya, 29, lipovskii@mail.ru

Dr. Valentina Zhurikhina, Russia, 195251, St.Petersburg, Polytechnicheskaya, 29, zhurikhina\_vv@spbstu.ru

### Abstract

We present studies of the formation of silver nanoparticles (NPs) in silver-sodium ion-exchanged glasses by a combination of thermal poling and nanosecond pulsed laser irradiation at 355 nm. In poling, silver ions drift deeper into the glass and become separated from the glass surface by a poled layer depleted in cations. Performed measurements have indicated poling-induced broadening of silver ions depth distribution. Laser irradiation reduces silver ions to atomic silver via breaking silver – non-bridging oxygen bonds, extraction of electrons from the non-bridging oxygen atoms and capturing these electrons and electrons generated via multi-photon absorption in the glass by silver ions. The depleted layer limits diffusion of silver atom towards glass surface and, as a consequence, formation of silver NPs on the surface of poled glasses. It is shown that thermal poling mode allows one to control formation of silver NPs of glass surface.

### Keywords:

Glass poling, surface metallization, silver nanoparticles, ion-exchange, laser inscribing

## 1 Introduction

Laser-assisted surface treatment has become a powerful tool for the formation of metal nanoparticles (NPs) in optically transparent media, primarily in glasses, and for the modification of glass-metal nanocomposites. The interest in metal NPs, located in the bulk or on the surface of a material, is due to their optical properties at surface plasmon resonance (SPR) wavelength, which provide selective optical absorption [1], high optical nonlinearity [2], enhanced Raman scattering [3], luminescence [4] and catalytic activity [5]. The control over NPs formation allows effective managing of the SPR spectral position and magnitude, which determine optical properties of individual NPs or glass-metal nanocomposites as a whole. In particular, laser-induced shape modification of NPs results in breaking central symmetry. This allows for alterations of the NPs resonant wavelength [1] and increased nonlinearity [6,7]. Additionally, it is possible to modify glass-metal nanocomposites via selective laser softening and melting of the glass matrix containing absorbing NPs [8].

The growth of NPs in silver-doped glasses under UV [9,10], visible [11] and near IR [12,13] irradiation using both continuous [14] and pulsed laser sources was reported, as well as the laser-induced deformation of NPs [15]. These studies were performed in the pulse duration domain from femtoseconds [16] to nanoseconds [17]. In most of the published studies, except for [10] and [13], silver ions were introduced in the glass matrix using the ion-exchange technique. This provided relatively high concentration of the embedded silver in the subsurface layer of glass [18], and the NPs formation in this layer was controlled by the laser irradiation parameters [10,15]. Figure 1 shows an example of the image directly written by a laser beam in a silver-sodium ion-exchanged silicate glass. This technique enables production of a large variety of optical elements, such as 2D structured optical amplitude masks, elements for data recording and storage, etc., with the spatial resolution determined by the laser beam diameter [19,20]. While the laser wavelength and fluence to a certain extent affect the kinetics of NP formation, control of the subsurface region properties of the glass, such as chemical composition, should allow additional control over NPs formation and modification [21]. For example, the dissolution of formed NPs and control over their formation via thermal poling were demonstrated in the case of hydrogen reduction of silver ions in ion-exchanged glasses [22,23]. In this paper, we present the controlled formation of silver NPs in ion-exchanged glass using a combination of thermal poling and nanosecond pulsed laser irradiation at 355 nm.

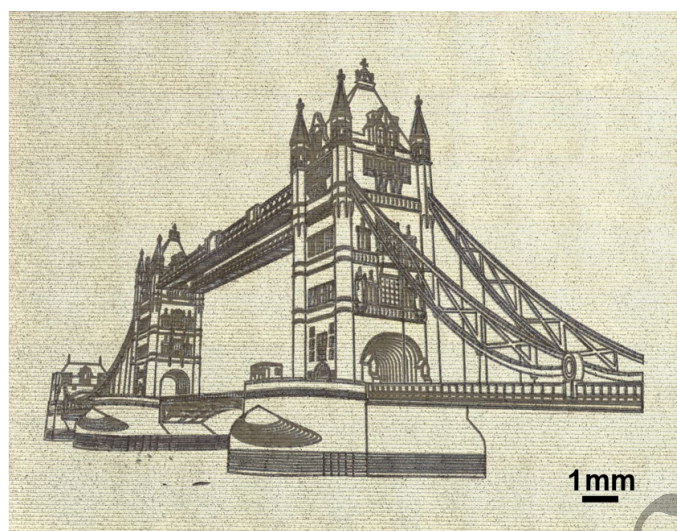


Figure 1. High-resolution optical microscopy image of Tower Bridge recorded in a silver-to-sodium ion-exchanged glass by laser irradiation.

## 2 Experimental

Soda-lime glass slides (72.2%wt.  $\text{SiO}_2$ , 14.3%wt.  $\text{Na}_2\text{O}$ , 1.2%wt.  $\text{K}_2\text{O}$ , 6.4%wt.  $\text{CaO}$ , 4.3%wt.  $\text{MgO}$ , 1.2%wt.  $\text{Al}_2\text{O}_3$ , 0.3%wt.  $\text{SO}_3$ , 0.03%wt.  $\text{Fe}_2\text{O}_3$  and 0.07%wt. of others, according to the producer data [24]) were ion-exchanged in silver-sodium melt solution: 5%wt.  $\text{AgNO}_3$ : 95%wt.  $\text{NaNO}_3$  for 20 min at 325°C. This led to the introduction of silver ions into the glass matrix. In the process, silver ions replaced sodium ions in several microns deep subsurface region of the glass, which shifted the position of the optical absorption edge. The change of optical absorption of the slides after the processing was characterized using Specord 50 spectrometer. In order to modify the glass and promote further silver ions penetration into the bulk of the sample, we thermally poled the ion-exchanged glass in air with pressed glassy carbon electrodes by applying DC voltage of 300 V at 300°C for 30 s to 2400s (40 min). The longest poling corresponded to the decay of the poling current down to 10% of its initial value. The fabricated samples were irradiated with a Nd:YVO<sub>4</sub> laser (Laservall Violino UV) with a pulse length of  $\tau = 10$  ns at a wavelength of  $\lambda = 355$  nm in standard atmospheric environment. The laser beam had a Gaussian intensity profile with  $M^2 < 1.3$ . The sample surface was irradiated with either focused or defocused laser beam, using a flat-field scanning lens system. The laser beam was raster scanned at a speed of 1 mm/s and a pulse repetition rate of 80 kHz (corresponding to 4800 pulses per spot) with the incident energy density (laser fluence) varied from 49 to 332 mJ/cm<sup>2</sup>. The irradiated areas were characterized with X-ray diffractometer D8 Discover (Cu K $\alpha$ ), an optical microscope (Olympus MX51-F), LEO 1550 Gemini scanning electron microscope (SEM), a hand-made optical system for extinction spectra measurement that included a halogen lamp (Ocean Optics HL-2000-FHSA-LL) as a light source and a modular spectrometer (Solar LS SC82) as a detector, the diameters of the illumination and collection light spots being 80 and 240  $\mu\text{m}$ , respectively. We also measured luminescence of the samples in spectral range of 620-660 nm (2700-3700  $\text{cm}^{-1}$ ) using confocal Raman microscope WITec Alpha 300R equipped with CW green laser (532 nm) and 100 $\times$ /0.9 objective. The system allowed measuring luminescence excited at different distances from the glass surface, vertical resolution being  $\sim 1$   $\mu\text{m}$ . The list of studied samples is presented in Table 1.

**Table 1.** The notations of studied samples.

Laser fluence, mJ/cm <sup>2</sup>	49	61	197	246	319	332
Poling duration						
Non-poled	0-49	0-61	0-197	0-246	0-319	0-332
30 s poling	-	-	1-197	1-246	1-319	1-332
90 s poling	2-49	2-61	2-197	2-246	2-319	2-332
2400 s poling	3-49	3-61	3-197	3-246	3-319	3-332

### 3 Results and Discussion

After irradiation of the prepared samples, we observed metallization of the laser-exposed glass region, similar to what we observed in silver-to-sodium exchanged glasses [25]. It should be noted that in the employed regimes of ion-exchange processing, silver ions do not penetrate in the glass deeper than 7  $\mu\text{m}$  [26]. Therefore, after the ion-exchange both sides of a glass slide contain silver ions enriched regions,  $\sim 7 \mu\text{m}$  thick each. These two relatively thin subsurface regions increase optical density of the processed sample at the irradiation wavelength by about 0.034. This is twice the initial optical density, as seen in Figure 2. Thus, the absorption in 7  $\mu\text{m}$  thick silver-doped region is half of the absorption of 1 mm-thick glass slide, which does not contain silver ions. That means that almost a quarter of the laser irradiation is absorbed by the silver-containing region under the irradiated surface of the sample. Besides, when the metallization begins, the absorption grows due to the absorption of formed NPs.

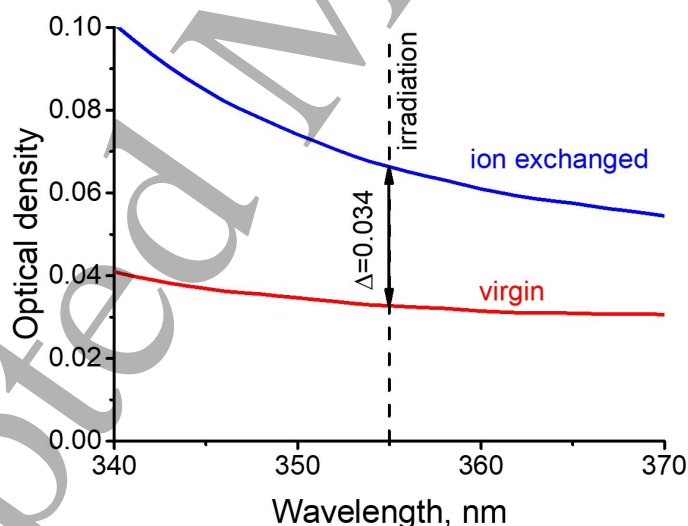


Figure 2. The change in optical absorption of the glass sample after the ion-exchange processing.

X-ray diffractometry (XRD) of the prepared samples demonstrated the presence of diffraction peaks, the positions of which correspond to the crystalline lattice of silver (see Figure 3). The average size of these nanocrystals evaluated in accordance with the peaks' width (see Figure 3) is not less than 27 nm. Unfortunately, it is hardly possible to use XRD data for exact evaluation of the NPs size, since ones formed in the bulk and on the surface of glass differ in size [27], and XRD returns the average value.

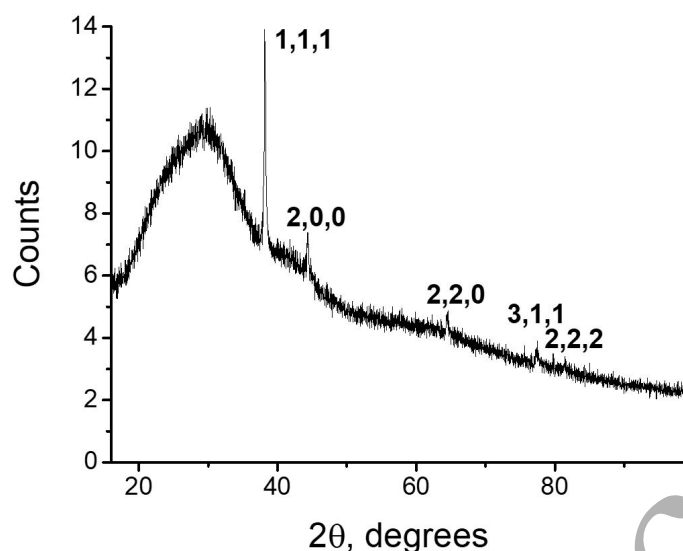


Figure 3. XRD of 2-319 sample. Positions of the peaks correspond to the crystalline planes of silver indicated above the peaks.

Following earlier reported mechanism of laser reduction of silver ions in glasses [28–33], we underline that the effect of laser irradiation on the silver-containing glass is two-fold. First, significant energy is transferred by nanosecond pulses and absorbed in the thin subsurface region of the glass (by both glass network formers and modifiers, including silver, bonded via non-bridging oxygen atoms [27]). This leads to heating of this region and its softening [28,29], as well as to the break of silver – non-bridging oxygen (NBO) bonds followed by the reduction of silver ions via extraction of electrons from NBO atoms [27]. Second, as established now [30–33], laser irradiation at 355 nm leads to free electrons formation in the glass due to multi-photon absorption. This, in turn, leads to the silver ion reduction to the metallic state via electron capturing. The oversaturation of the subsurface region of glass with silver atoms determines its tendency to phase decomposition [28].

There are two sinks for the “extra” silver atoms: the glass surface, which is a strong sink for silver reduced close to the surface, and silver atomic clusters formed in the bulk of the ion-exchange region [34]. These clusters are nuclei of silver NPs [35,36] and the preferred sink for silver atoms reduced deeper in the glass. Thus, phase decomposition in the bulk of the glass results in the appearance of silver atomic clusters  $Ag_n$  and then silver nanoparticles in the subsurface layer, while diffusion of silver atoms to the glass surface and their diffusion along the surface result in the formation of silver NPs on the glass surface [37]. Besides, an increase in the concentration of silver nanoparticles both in the subsurface region of the glass and on the surface is accompanied by a decrease in the concentration of silver ions and, respectively, silver atomic clusters in the subsurface region. Increasing the laser fluence leads to an increase in the concentration of neutral silver and its faster diffusion due to stronger heating of glass. This results in a faster growth of nanoparticles and an increase in metal volume fraction in the sample [25].

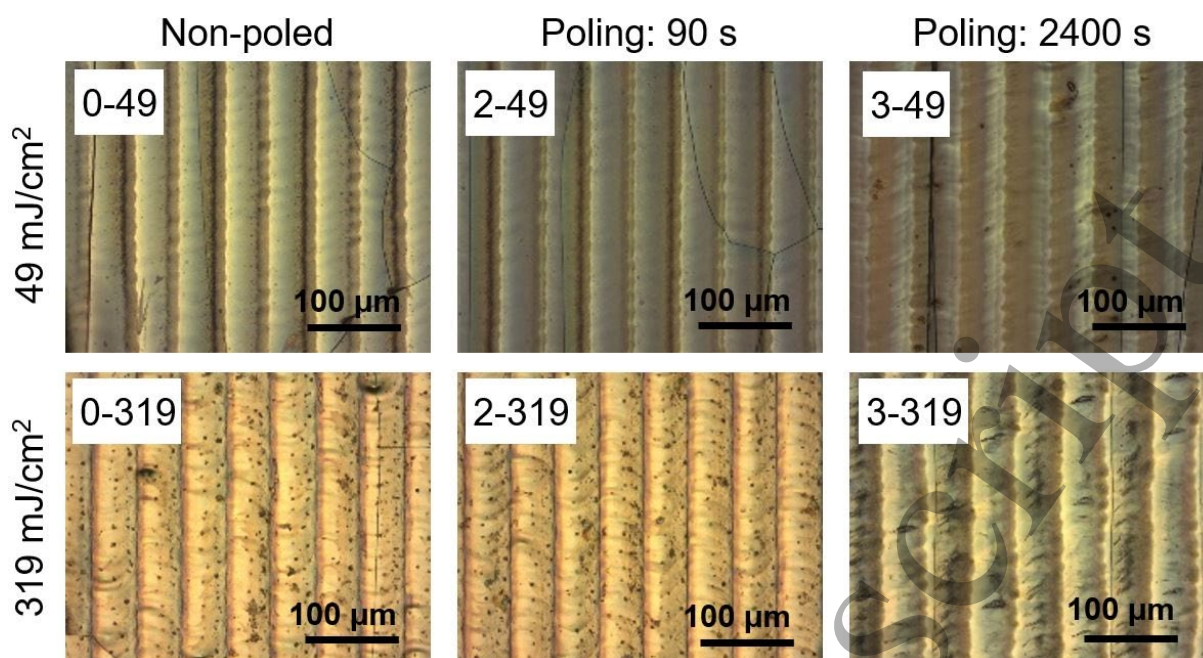
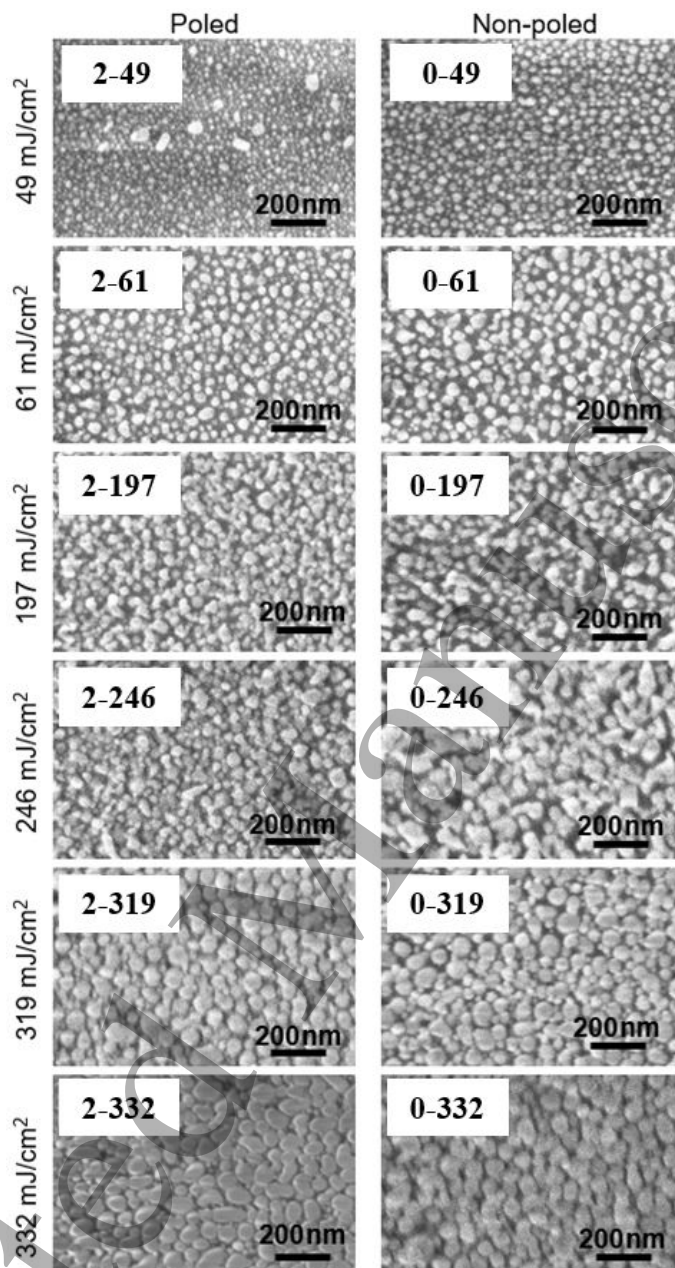


Figure 4. Optical microscopy images (20X magnification) of the samples marked in the photos according to Table 1.

Figure 4 presents the results of the optical microscopy of the laser-irradiated glass slides. Higher refractivity (brighter images) corresponds to higher metallization of the glass surface. One can clearly see the difference in the light reflection between poled (3-49 and 3-319) and non-poled (0-49 and 0-319) samples in Figure 4, which is due to a difference in the out-flow of the reduced silver to the surface. In the case of air-poling of a multicomponent glass with pressed anodic electrode, ions with higher mobility, including silver ions, drift into deeper regions of the glass, while less mobile alkaline-earth elements and hydrogen remain mainly in the subsurface region depleted in more mobile ions [38,39]. After the reduction, silver atoms move to the strongest sink, and for non-poled samples this is the glass surface. Surface diffusion of these atoms results in NPs formation. Glass poling, in turn, results in the formation of ions-depleted layer which does not contain silver (the thickness of this layer depends on the poling conditions). This layer separates most of the reduced silver atoms from the glass surface. Moreover, earlier it was shown that the poled layer limits the diffusion [26] because of low mobility of hydrogen [40] and alkaline-earth ions [41] present in this layer, as well as due to a decrease in the concentration of non-bridging oxygen bonds [42]. Therefore, the surface sink for silver atoms in a poled glass is weaker than in the non-poled one, and hence the flux of the atoms to the surface is less. The thicker depleted layer, the weaker the surface sink. Lower laser fluence initiates less intensive formation of neutral silver, which results in less effective formation of silver NPs. Thus, the longer the poling and the lower the laser fluence, the less is glass surface metallization, as illustrated by Figure 4. For 90 seconds poling, the difference between poled and non-poled samples exists for the lowest laser fluence ( $49 \text{ mJ/cm}^2$ ) only. The higher laser fluence,  $319 \text{ mJ/cm}^2$ , initiates more intensive formation and out-flow of neutral silver, which makes the difference between poled and non-poled glass negligible – compare samples 0-319 and 2-319. The longest (2400 seconds) poling of the glass leads to the strongest difference between poled (samples 3-49 and 3-319) and non-poled (0-49 and 0-319) irradiated samples due to a thicker depleted layer under the glass surface. The difference between the samples 0-49 and 3-49 can be seen “with the naked eye” in Figure 4. Increasing laser fluence weakens this



1  
2 difference because of more intensive formation of neutral silver and growth of nanoparticles in  
3 stronger heated glass, see samples 0-319 and 3-319 in Figure 4. At the same time, our SEM  
4 characterization (Figure 5) indicates that all studied samples contain differing in size and  
5 concentration nanoparticles on the surface.  
6



48  
49 Figure 5. Top view SEM images of the poled (90 sec) and non-poled samples after laser  
50 irradiation. Numbers of the samples are marked in the images according to Table 1.  
51

52 Since for the poled samples the glass surface is separated from the silver atoms by a depleted  
53 layer, the concentration of silver NPs on the surface of these samples is less (compare samples  
54 2-49 – 2-332 and 0-49 – 0-332 in Figure 5). However, all samples contain silver NPs of 10 to  
55 80 nm in size on the surface after the laser irradiation. One can see that the radius and volume  
56 fraction of metal NPs grow with the increase of the laser fluence (from 2-49 to 2-319, and  
57 from 0-49 to 0-319 in Figure 5), which is caused by more intense reduction of silver ions. It is  
58 important to note the exceptions in 2-332 and 0-332 in Figure 5, corresponding to the highest  
59 laser fluence used in the experiment, 332 mJ/cm<sup>2</sup>. Here one can see a change in the NPs  
60

shape, which is more pronounced for a poled sample. This shape transformation is supposedly due to a heating of absorbing metal NPs by the laser. Thus, one can see in Figure 5 that thermal poling makes it possible to change the parameters of laser-formed silver NPs on the glass surface affecting both their size and shape. This is illustrated by the absorption spectra of the samples presented in Figure 6.

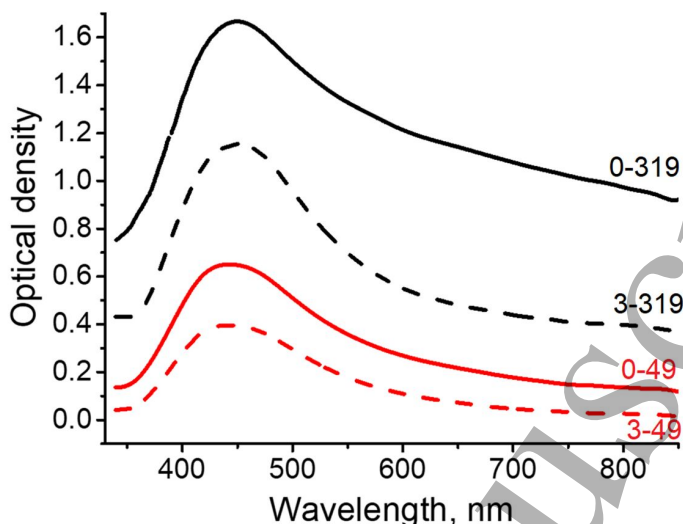


Figure 6. Spectra of the non-poled (solid) and poled (dashed) samples. The poling duration is 2400 s. The laser fluence ( $\text{mJ}/\text{cm}^2$ ) is indicated near the plots.

All spectra demonstrate a peak of absorption at the wavelength of  $\sim 430$  nm, corresponding to the plasmon resonance of silver NPs. An increase in the laser fluence leads to an increase in the volume fraction of the NPs and, as a consequence, to an increase in optical absorption. The modification and partial destruction of NPs at higher laser fluence,  $319 \text{ mJ}/\text{cm}^2$ , manifests itself through a change in the shape of the longer-wavelengths shoulder of the absorption peak, and this is more pronounced in stronger absorbing non-poled sample [43].

Other experimental conditions being equal, optical absorption of poled samples is less than the absorption of non-poled ones despite similar content of silver in the glass. Thus, the poled samples contain less NPs. In Figure 7 we show the intensity of luminescence (integrated over the range  $2700\text{-}3700 \text{ cm}^{-1}$ ) of the ion-exchanged glass, ion-exchanged glass irradiated with  $332 \text{ mJ}/\text{cm}^2$  laser fluence, ion-exchanged glass poled for 2400 s, and ion-exchanged poled glass irradiated with the same laser fluence of  $332 \text{ J}/\text{cm}^2$ . The luminescence in this frequency range can be attributed to small silver clusters  $\text{Ag}_2\text{-Ag}_4$  present in the ion-exchanged region of the glass, which are typical for silver ion-exchanged glasses [44–46].

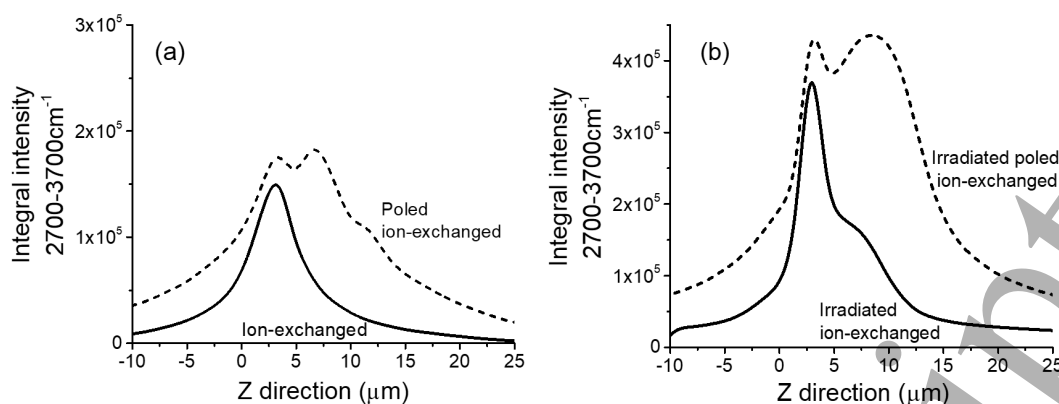


Figure 7. The depth distribution of the integral intensity of luminescence corresponding to silver clusters  $\text{Ag}_2\text{-Ag}_4$  in the subsurface region of (a) ion-exchanged glass and poled for 2400 s ion-exchanged glass, and (b) ion-exchanged glass irradiated at  $332 \text{ mJ/cm}^2$  laser fluence and poled ion-exchanged glass irradiated by the same laser fluence.  $Z=0$  nominally corresponds to the sample surface, and  $Z>0$  - to the subsurface region.

In Figure 7a one can see that the thickness of the region containing silver clusters in poled ion-exchanged glass exceeds one in non-poled glass, thus, thermal poling leads to a broadening of silver ions depth distribution. This corresponds to a decrease in silver concentration, which should reduce the probability of the formation of NPs. This is well illustrated by the measurements of  $\text{Ag}_2\text{-Ag}_4$  luminescence after laser irradiation (Figure 7b). In the laser-irradiated poled and non-poled samples, one can see a sharp peak corresponding to the glass subsurface region containing numerous silver clusters. Deeper in the sample, for poled glass there is a second peak that reflects the presence of highly concentrated silver clusters. However, for non-poled glass, such a peak is practically absent, and only a shoulder follows the main surface luminescence peak. Moreover, the integrated luminescence is essentially stronger in poled glass, that indicates higher concentration of both  $\text{Ag}_2\text{-Ag}_4$  clusters (neutral silver) and, supposedly, silver ions. Consequently, less silver is concentrated in the nanoparticles after the irradiation of the poled sample. This is due to deeper distribution of silver ions after the poling. The local minimum in the depth distribution of luminescence in the laser-irradiated poled glass in Figure 7b supposedly corresponds to silver-depleted poled region. It is worth to note that the measured distribution of  $\text{Ag}_2\text{-Ag}_4$  luminescence intensity is very similar to the registered with secondary ion mass spectroscopy distribution of sodium ions in poled glasses after heat treatment [47], which indicated the diffusion of sodium ions through ion-depleted region towards the glass surface. This similarity indirectly confirms the conclusion from the luminescence measurements on the distribution of silver ions.

It should be mentioned that the depth scan of the luminescence provides just qualitative information because the excitation of the luminescence takes place not only in the focal region but also out of the objective focus. Additionally, since diffusive growth of NPs is the most intensive at the strongest sink, that is the surface for silver atoms placed in the subsurface region of the glass (see Figure 2 in [27]), the poling-depleted layer also weakens the NPs formation.

Along with the NPs formation, the laser irradiation resulted in stress-induced modification of the subsurface layer of the glass, as shown by SEM image presented in Figure 8. For  $197 \text{ mJ/cm}^2$  laser fluence and 30 s poling duration, the thickness of this layer is about  $100 \mu\text{m}$  while our ion exchange conditions provided silver ions penetration depth about  $7 \mu\text{m}$  [26].

Thus, the 100  $\mu\text{m}$  thick modified layer is due to the fast heating through the absorption of the laser radiation by several microns-thick ion-exchanged region of glass and by silver NPs after their formation, the latter is evidenced by the absorption spectra presented in [25]. Since the formation of absorbing NPs is the result of the irradiation, the highest temperature should be reached just before moving the irradiating laser beam to the next position. This is because the high frequency of the laser pulses keeps the glass heated and supposedly soften/melted [28] between subsequent pulses. Thus, rapid cooling of the irradiated spot immediately after the irradiation leads to significant stresses because of the difference in thermal expansion of the heated region and the bulk of the glass.

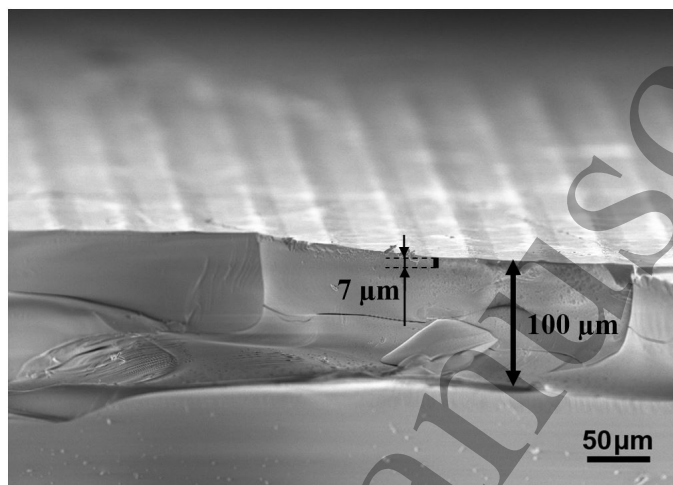


Figure 8. Cross-section SEM image of 1-197 sample.

#### 4 Conclusions

It is shown that laser-assisted formation of silver nanoparticles in glass enriched with silver ions via classic ion-exchange from the molten salt can be controlled in two ways: by glass polishing before nanosecond UV laser irradiation, and by the laser parameters. Combination of these methods allows for controlled formation of nanoparticles on glass surface and also in the depth of glass. This paves the way for further development of new materials with special characteristics using laser treatment and opens up a variety of applications in photonics, such as waveguides and plasmonic structures.

#### Acknowledgements

The research is funded by the Ministry of Science and Higher Education of the Russian Federation as a part of World-class Research Center program: Advanced Digital Technologies [contract No. 075-15-2020-934 dated 17.11.2020]. I.R. thanks The Academy of Finland Mobility Grant, The Saastamoinen Foundation, and Academy of Finland Flagship PREIN. E.B. thanks the Council for Grants of the President of the Russian Federation [project SP-1491.2021.4].

## References

- [1] Kelly K L, Coronado E, Zhao L L and Schatz G C 2003 The Optical Properties of Metal Nanoparticles: The Influence of Size, Shape, and Dielectric Environment *J. Phys. Chem. B* **107** 668–77
- [2] Voisin C, Del Fatti N, Christofilos D and Vallée F 2001 Ultrafast Electron Dynamics and Optical Nonlinearities in Metal Nanoparticles *J. Phys. Chem. B* **105** 2264–80
- [3] Willets K A and Van Duyne R P 2007 Localized Surface Plasmon Resonance Spectroscopy and Sensing *Annu. Rev. Phys. Chem.* **58** 267–97
- [4] Kulakovich O, Strekal N, Yaroshevich A, Maskevich S, Gaponenko S, Nabiev I, Woggon U and Artemyev M 2002 Enhanced Luminescence of CdSe Quantum Dots on Gold Colloids *Nano Lett.* **2** 1449–52
- [5] Liu Z, Hou W, Pavaskar P, Aykol M and Cronin S B 2011 Plasmon Resonant Enhancement of Photocatalytic Water Splitting Under Visible Illumination *Nano Lett.* **11** 1111–6
- [6] Chervinskii S, Koskinen K, Scherbak S, Kauranen M and Lipovskii A 2018 Nonresonant Local Fields Enhance Second-Harmonic Generation from Metal Nanoislands with Dielectric Cover *Phys. Rev. Lett.* **120** 113902
- [7] Zolotovskaya S A, Tyrk M A, Stalmashonak A, Gillespie W A and Abdolvand A 2016 On second harmonic generation and multiphoton-absorption induced luminescence from laser-reshaped silver nanoparticles embedded in glass *Nanotechnology* **27** 435703
- [8] Antonov I, Bass F, Kaganovskii Y, Rosenbluh M and Lipovskii a. 2003 Fabrication of microlenses in Ag-doped glasses by a focused continuous wave laser beam *J. Appl. Phys.* **93** 2343
- [9] Goutaland F, Sow M, Ollier N and Vocanson F 2012 Growth of highly concentrated silver nanoparticles and nanoholes in silver-exchanged glass by ultraviolet continuous wave laser exposure *Opt. Mater. Express* **2** 350
- [10] Wackerow S and Abdolvand A 2014 Generation of silver nanoparticles with controlled size and spatial distribution by pulsed laser irradiation of silver ion-doped glass *Opt. Express* **22** 5076
- [11] Blondeau J P, Pellerin S, Vial V, Dzierżęga K, Pellerin N and Andreatza-Vignolle C 2008 Influence of pulsed laser irradiation on precipitation of silver nanoparticles in glass *J. Cryst. Growth* **311** 172–84
- [12] Dai Y, Yu G, He M, Ma H, Yan X and Ma G 2011 High repetition rate femtosecond laser irradiation-induced elements redistribution in Ag-doped glass *Appl. Phys. B* **103** 663–7
- [13] Babich E, Kaasik V, Redkov A, Maurer T and Lipovskii A 2020 SERS-Active Pattern in Silver-Ion-Exchanged Glass Drawn by Infrared Nanosecond Laser *Nanomaterials* **10** 1849
- [14] Tite T, Ollier N, Sow M C, Vocanson F and Goutaland F 2017 Ag nanoparticles in soda-lime glass grown by continuous wave laser irradiation as an efficient SERS platform for pesticides detection *Sensors Actuators, B Chem.* **242** 127–31

- 1  
2  
3  
4  
5  
6  
7  
8  
9  
10  
11  
12  
13  
14  
15  
16  
17  
18  
19  
20  
21  
22  
23  
24  
25  
26  
27  
28  
29  
30  
31  
32  
33  
34  
35  
36  
37  
38  
39  
40  
41  
42  
43  
44  
45  
46  
47  
48  
49  
50  
51  
52  
53  
54  
55  
56  
57  
58  
59  
60
- [15] Podlipensky A, Abdolvand A, Seifert G and Graener H 2005 Femtosecond laser assisted production of dichroitic 3D structures in composite glass containing Ag nanoparticles *Appl. Phys. A* **80** 1647–52
- [16] Almeida J M P, Ferreira P H D, Manzani D, Napoli M, Ribeiro S J L and Mendonça C R 2014 Metallic nanoparticles grown in the core of femtosecond laser micromachined waveguides *J. Appl. Phys.* **115** 193507
- [17] Cattaruzza E, Mardegan M, Trave E, Battaglin G, Calvelli P, Enrichi F and Gonella F 2011 Modifications in silver-doped silicate glasses induced by ns laser beams *Appl. Surf. Sci.* **257** 5434–8
- [18] Liñares J, Sotelo D, Lipovskii A A A, Zhurikhina V V V., Tagantsev D K K and Turunen J 2000 New glasses for graded-index optics: influence of non-linear diffusion in the formation of optical microstructures *Opt. Mater. (Amst)*. **14** 145–53
- [19] Abou Khalil A, Bérubé J P, Danto S, Desmoulin J C, Cardinal T, Petit Y, Vallée R and Canioni L 2017 Direct laser writing of a new type of waveguides in silver containing glasses *Sci. Rep.* **7** 1–9
- [20] Wackerow S and Abdolvand A 2012 Laser-assisted one-step fabrication of homogeneous glass–silver composite *Appl. Phys. A* **109** 45–9
- [21] Fleming L A H, Tang G, Zolotovskaya S A and Abdolvand A 2014 Controlled modification of optical and structural properties of glass with embedded silver nanoparticles by nanosecond pulsed laser irradiation *Opt. Mater. Express* **4** 969
- [22] Lipovskii A A, Rusan V V. and Tagantsev D K 2010 Imprinting phase/amplitude patterns in glasses with thermal poling *Solid State Ionics* **181** 849–55
- [23] Chervinskii S, Sevriuk V, Reduto I and Lipovskii A 2013 Formation and 2D-patterning of silver nanoisland film using thermal poling and out-diffusion from glass *J. Appl. Phys.* **114** 224301
- [24] Soda-lime glass slides composition, (n.d.) 2021.07.21. <https://www.agarscientific.com/microscope-slides.html>.
- [25] Reduto I, Wackerow S, Zolotovskaya S, Abdolvand A, Lipovskii A and Svirko Y 2020 Nanosecond laser surface silver metallization of wet ion exchanged glasses *J. Phys. Conf. Ser.* **1461** 012136
- [26] Babich E, Reduto I, Redkov A, Reshetov I, Zhurikhina V and Lipovskii A 2020 Thermal poling of glasses to fabricate masks for ion exchange *J. Phys. Conf. Ser.* **1695** 012107
- [27] Redkov A, Chervinskii S, Baklanov A, Reduto I, Zhurikhina V and Lipovskii A 2014 Plasmonic molecules via glass annealing in hydrogen *Nanoscale Res. Lett.* **9**
- [28] Rosenbluh M, Antonov I, Ianetz D, Kaganovskii Y and Lipovskii A A 2003 Microfabrication of structures by laser light in metal-doped glasses *Opt. Mater. (Amst)*. **24** 401–10
- [29] Delgado T, Nieto D and Flores-Arias M T 2016 Soda-lime glass microlens arrays fabricated by laser: Comparison between a nanosecond and a femtosecond IR pulsed laser *Opt. Lasers Eng.* **86** 29–37

- 1  
2  
3  
4  
5  
6  
7  
8  
9  
10  
11  
12  
13  
14  
15  
16  
17  
18  
19  
20  
21  
22  
23  
24  
25  
26  
27  
28  
29  
30  
31  
32  
33  
34  
35  
36  
37  
38  
39  
40  
41  
42  
43  
44  
45  
46  
47  
48  
49  
50  
51  
52  
53  
54  
55  
56  
57  
58  
59  
60
- [30] Hongo T, Sugioka K, Niino H, Cheng Y, Masuda M, Miyamoto I, Takai H and Midorikawa K 2005 Investigation of photoreaction mechanism of photosensitive glass by femtosecond laser *J. Appl. Phys.* **97** 063517
- [31] Marquestaut N, Petit Y, Royon A, Mounaix P, Cardinal T and Canioni L 2014 Three-Dimensional Silver Nanoparticle Formation Using Femtosecond Laser Irradiation in Phosphate Glasses: Analogy with Photography *Adv. Funct. Mater.* **24** 5824–32
- [32] Royon A, Petit Y, Papon G, Richardson M and Canioni L 2011 Femtosecond laser induced photochemistry in materials tailored with photosensitive agents [Invited] *Opt. Mater. Express* **1** 866
- [33] Jipa F, Iosub S, Calin B, Axente E, Sima F and Sugioka K 2018 High Repetition Rate UV versus VIS Picosecond Laser Fabrication of 3D Microfluidic Channels Embedded in Photosensitive Glass *Nanomaterials* **8** 583
- [34] Nedyalkov N, Dikovska A, Koleva M, Stankova N, Nikoy R, Borisova E, Genova T, Aleksandrov L, Iordanova R and Terakawa M 2020 Luminescence properties of laser-induced silver clusters in borosilicate glass *Opt. Mater. (Amst)*. **100** 109618
- [35] Kaganovskii Y, Lipovskii A, Rosenbluh M and Zhurikhina V 2007 Formation of nanoclusters through silver reduction in glasses: The model *J. Non. Cryst. Solids* **353** 2263–71
- [36] Simo A, Polte J, Pfänder N, Vainio U, Emmerling F and Rademann K 2012 Formation Mechanism of Silver Nanoparticles Stabilized in Glassy Matrices *J. Am. Chem. Soc.* **134** 18824–33
- [37] Petit Y, Danto S, Guérineau T, Khalil A A, Lé Camus A, Fargin E, Duchateau G, Bérubé J-P P, Vallée R, Messaddeq Y, Cardinal T, Canioni L, Abou Khalil A, Le Camus A, Fargin E, Duchateau G, Bérubé J-P P, Vallée R, Messaddeq Y, Cardinal T and Canioni L 2018 On the femtosecond laser-induced photochemistry in silver-containing oxide glasses: Mechanisms, related optical and physico-chemical properties, and technological applications *Adv. Opt. Technol.* **7** 291–309
- [38] Dergachev A, Kaasik V, Lipovskii A, Melehin V, Redkov A, Reshetov I and Tagantsev D 2020 Control of soda-lime glass surface crystallization with thermal poling *J. Non. Cryst. Solids* **533** 11989
- [39] Lepienski C M, Giacometti J A, Leal Ferreira G F, Freire F L and Achete C A 1993 Electric field distribution and near-surface modifications in soda-lime glass submitted to a dc potential *J. Non. Cryst. Solids* **159** 204–12
- [40] Doremus R H 2005 Mechanism of electrical polarization of silica glass *Appl. Phys. Lett.* **87** 232904
- [41] Mehrer H, Imre A W and Tanguet-Nijokep E 2008 Diffusion and ionic conduction in oxide glasses *J. Phys. Conf. Ser.* **106** 012001
- [42] Redkov A V, Melehin V G and Lipovskii A A 2015 How Does Thermal Poling Produce Interstitial Molecular Oxygen in Silicate Glasses? *J. Phys. Chem. C* **119** 17298–307
- [43] Wang Y-L, Nan F, Liu X-L, Zhou L, Peng X-N, Zhou Z-K, Yu Y, Hao Z-H, Wu Y, Zhang W, Wang Q-Q and Zhang Z 2013 Plasmon-Enhanced Light Harvesting of

1  
2 Chlorophylls on Near-Percolating Silver Films via One-Photon Anti-Stokes  
3 Upconversion *Sci. Rep.* **3** 1861  
4

- 5 [44] Eichelbaum M, Rademann K, Hoell A, Tatchev D M, Weigel W, Stöber R and  
6 Pacchioni G 2008 Photoluminescence of atomic gold and silver particles in soda-lime  
7 silicate glasses *Nanotechnology* **19** 135701  
8  
9 [45] Dubrovin V D, Ignatiev A I, Nikonorov N V., Sidorov A I, Shakhverdov T A and  
10 Agafonova D S 2014 Luminescence of silver molecular clusters in photo-thermo-  
11 refractive glasses *Opt. Mater. (Amst)*. **36** 753–9  
12  
13 [46] Nedyalkov N, Dikovska A, Koleva M, Stankova N, Nikov R, Borisova E, Genova T,  
14 Aleksandrov L, Iordanova R and Terakawa M 2020 Luminescence properties of laser-  
15 induced silver clusters in borosilicate glass *Opt. Mater. (Amst)*. **100** 109618  
16  
17 [47] Redkov A V, Melehin V G, Raskhodchikov D V, Reshetov I V, Tagantsev D K,  
18 Zhurikhina V V and Lipovskii A A 2019 Modifications of poled silicate glasses under  
19 heat treatment *J. Non. Cryst. Solids* **503–504** 279–83  
20  
21  
22  
23  
24  
25  
26  
27  
28  
29  
30  
31  
32  
33  
34  
35  
36  
37  
38  
39  
40  
41  
42  
43  
44  
45  
46  
47  
48  
49  
50  
51  
52  
53  
54  
55  
56  
57  
58  
59  
60